ORIGINAL ARTICLE

Unsteady Solute Dispersion in Jeffrey Blood Flow with the Effect of Stenosis

Aina Fariha Yusof [1], Nurul Aini Jaafar [1]*, Mallinath Dhange [2,3]

[1] Department of Mathematical Sciences, Faculty of Science, Universiti Teknologi Malaysia, 81310 UTM Johor Bahru, Johor, Malaysia
[2] Department of Mathematics, BLDEA's VP Dr. PG Halakatti College of Engineering and Technology, Vijayapur,586103 India (Affiliated to Visvesvaraya Technological University, Belagavi, Karnataka, India)
[3] Department of Allied Health Sciences, Shri B.M. Patil Medical College, Hospital and Research Centre, BLDE (Deemed to be University), Vijayapur, India

ABSTRACT

Introduction: The research aims to analyst the impact of the ratio of relaxation time, slip velocity and the relative height of stenosis towards the blood velocity and solute dispersion in the Jeffrey blood flow within a stenosed artery. **Methods:** Generalized Dispersion Model (GDM) is applied into the convective diffusion equation which is then solved to obtain solute concentration and dispersion function. **Results and Discussion:** When the relative stenosis height increases, there is a slight reduction in blood flow velocity. As time increases, the unsteady dispersion function contracts at the center and expands along the arterial wall. With an increases in the ratio of relaxation time, the dispersion function expands along the arterial wall and contracts at the center. **Conclusion:** The presence of the ratio of relaxation time in a stenosed artery can disrupt both blood velocity and the dispersion function. This research has the potential to predict drug delivery to specific stenosed regions, thereby enabling more precise and targeted medical treatment.
Malaysian Journal of Medicine and Health Sciences (2025) 21(s2): 98–107. doi:10.47836/mjmhs.21.s2.15

Keywords: Jeffrey fluid, Blood flow, Drug dispersion, Ratio of relaxation time, Stenosis

Corresponding Author:
Nurul Aini Jaafar
Email: nurulaini.jaafar@utm.my
Handphone No: +60108342991

INTRODUCTION

Cardiovascular diseases (CVDs) are one of the most disease that had received much attention throughout the year and the leading cause of death globally. Medications are administered into the bloodstream to address these issues including the treatment of stenosis. The narrowing of blood vessels, known as stenosis, is typically caused by the buildup of plaque or the thickening of the arterial walls. This condition can significantly impede blood flow, leading to various cardiovascular complications. Improving the treatment of CVD is vital for tackling this problem, as inaccuracies in treatment administration can disrupt the effectiveness of the drug. Therefore, mathematical modeling, specifically in the field of fluid mechanics, is crucial to study and understand the effectiveness of medications in the bloodstream. Most researchers studied on the solute dispersion in blood flow is essential to enhance the effectiveness of CVD treatments and ultimately reduce the impact of these diseases on global health. The goal of the previous studies was to ensure that medications are administered accurately to maximize their effectiveness in treating CVD including stenosis.

The study of Non-Newtonian fluids is a key area in science and engineering for understanding how blood behaves. Understanding the non-Newtonian behavior of blood is crucial for studying hemodynamics, which is the science of blood flow through the circulatory system. Non-Newtonian fluid model is essential for designing and optimizing medical devices such as artificial hearts, blood pumps, and stents. These devices must operate effectively within the dynamic, non-Newtonian flow environment of the bloodstream. Accurate modeling of blood behavior ensures that these devices are safe and efficient. It allows researchers and medical professionals to understand the complex dynamics of blood flow, leading to advancements in diagnosing and treating cardiovascular diseases and creating more effective medical interventions and devices.

Among the various non-Newtonian fluid models, the Jeffrey fluid model has garnered significant attention from researchers due to its suitability for representing physiological fluids. The Jeffrey's fluid model is characterized as a non-Newtonian fluid that possessing the

characteristics of shear thinning, where the fluid's viscosity decreases with an increasing shear stress rate (1). Other than that, the Jeffrey fluid model can capture the stress relaxation behavior of non-Newtonian fluids, a feature that the conventional viscous fluid model cannot describe (2). The ratio of relaxation time, often known as Jeffrey fluid parameter is a parameter that use in rheology to examine the behavior of viscoelastic. In terms of viscoelasticity, this material expresses both elastic (solid-like) and viscous (liquid-like) properties, and their reaction to an applied stress depending on the time scale of the alteration and the relaxation of internal stresses. The relaxation time is a measure of how long it takes for a substance to relax and return to its original state after being subjected to an external force or change. Then, the ratio of relaxation time also refers to the proportion between the longest and shortest relaxation times in a viscoelastic material. The Jeffrey fluid model is acknowledged as a more general form of the commonly used models of non-Newtonian fluids, as its constitutive equation can be transformed into the Newtonian model's equation in specific conditions.

The research by Khan et al. (3) focused on the peristaltic movement of a Jeffrey fluid within an asymmetric channel with the changing viscosity in a porous mode. Priyadharshini and Ponalagusamy (4) examined an unsteady stenosed tapered artery stenosis for two-blood flow fluid model, by considering variable viscosity with the effect of a magnetic field. This study considered plasma in the outer layer acts as a Newtonian fluid while the blood in the central region pursues the Jeffrey fluid model. Chauhan and Tiwari researched the effects of variable viscosity and the Jeffrey fluid model on solute dispersion within microvessels, such as arterioles, venules, and capilaries, incorporating wall absorption.

Studying stenosis holds great significance in the realm of cardiovascular health. Employing mathematical modeling in fluid mechanics to investigate stenosis offers invaluable insights into the intricate hemodynamics linked to constricted blood vessels. The Carreau blood flow through tapered artery stenosis was investigated by Akbar and Nadeem (6). The blood flow model was represented through an axially asymmetrical but radially symmetrical stenosis. Yan et al. (7) examined how different cone angles of stenosis affect Sisko non-Newtonian blood flow, considering the influence of applied thermal heat flux. Dhange et al. (8) investigated the blood flowing through an inclined stenotic blood vessel which reduces the arterial side and generates an aneurysm, treated the blood as Casson fluid. Munir et al. (9) examined the artery affected by stenosis, considering arterial inclination and the acceleration factor of body forces by treating the blood as Herschel-Bulkley. Dhange et al. (10) examined the impact of overlapping stenosis on Casson fluid flow under mild stenosis conditions. Shukla et al. (11) examined the impact of shear stress on the arterial wall in artery and narrowing of the artery on blood flow. They approached this by modeling the blood as power-law and Casson-model fluids. Their study analyzed about how these different fluids models behave in the presence of stenosis. Hussain et al. (12) explored the steady-state flow of an incompresible fluid, specially treated as a Williamson fluid, passing through a stenosed region characterized by a cosine constriction The steady two-dimensional flow of a power-law fluid through vertically asymmetric and symmetric narrowings was examined by Owasit and Sriyab (13). The vertically asymmetric stenosis is defined by a distinctive shape that merges features of a bell curve and a cosine curve. This shape features a first half that is either a bell or cosine curve, with the second half taking on an alternative form.

By using Generalized Dispersion Method, Ratchagar and Vijayakumar (14) studied the dispersion of a solute in a non-Newtonian couple stress fluid flow within an inclined channel flanked by porous beds. Singh and Murthy (15) investigated the unsteady of solutes dispers in pulsatile flows of Newtonian and non-Newtonian K-L fluids through a circular tube, utilizing higher-order moments. Das et al. (16) studied the dispers of solute in a pulsatile non-Newtonian Carreau-Yasude fluid flow through a tube with narrow walls, with the impact of irreversible and reversible interactions with the wall and focusing on both short and long time scales.

It appears that the role of relaxation time and stenosis height in solute dispersion within Jeffrey fluid bloodstreams has been largely neglected. Most of previous studies have concentrated on solute dispersion in blood flow, ignoring the potential effects of relaxation time and stenosis. This research formulates the Jeffrey fluid model to mathematically explore steady blood flow, considering the impacts of the relaxation time ratio, the stenosis profile relative height, and slip velocity within a narrowed artery. The velocity slip phenomenon arises from the varying rheological properties of blood components. Slip velocity in blood flow refers to the difference in velocity between the blood and the inner lining of blood vessels. The plasma layer, being less viscous compared to the blood cells, tends to flow faster along the vessel wall. As a result, a velocity gradient is formed across the blood flow, with the highest velocity occurring in the plasma layer and gradually decreasing towards the center of the vessel. To describe the entire dispersion process, the General Dispersion Model is employed to solve the convective-diffusion equation that introduced by Gill and Sankarasubramaniam (17). Jeffrey fluid is chosen for this research because it provides a better understanding for analyzing the ratio of relaxation time. Hence, from this research, the medicine can be administered accurately for the blood that exhibits the characteristic of a Jeffrey fluid.

MATERIALS AND METHODS

Mathematical Formulation

The treatment of blood as a Jeffrey fluid in a straight circular pipe (artery) is addressed in the present study, where the geometry is considered to show cylindrical, axisymmetric, laminar, and fully developed unidirectional flows of a viscous incompressible fluid in the axial direction Shown in Fig. 1 is the geometry of solute dispersion in blood flow through a stenosed artery in Jeffrey fluid, with the constant radius of the straight artery in the non-stenotic region represented by $\overline{R}_0$, the length of stenosis marked by, $\overline{L}_0$ the stenosis location indicated by $\overline{d}$, and the maximum height of the stenosis denoted by $\overline{\delta}_h$, which is assumed to be much smaller compared to the radius of the stenosed artery $\overline{R}_0$. Using a cylindrical polar coordinate system $(\overline{r},\overline{\theta},\overline{z})$ the blood flow in an artery is analyzed, with $\overline{r}$ as the radius, $\overline{\theta}$ as the azimuthal angle, and $\overline{z}$ as the axial coordinates. Consideration is given to the effects of the relaxation time ratio and the relative height of the stenosis profile through a stenosed artery.

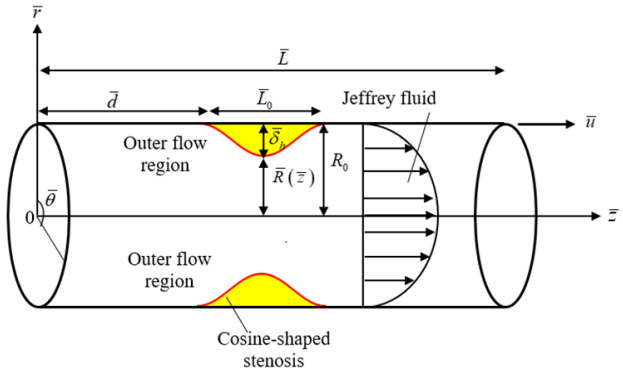

Fig 1: The geometry of dispersion of solute in blood flow through stenosed artery in Jeffrey fluid.

the constitutive equation of Jeffrey fluid is given by (5)

$$\overline{\tau}=\frac{1}{1+\lambda}\left[\overline{\mu}_J\left(-\frac{d\overline{u}}{d\overline{r}}\right)\right], 0\le\overline{r}\le\overline{R}(\overline{z}), \tag{1}$$

where $\overline{\tau}$ is the shear stress, u is the velocity, $\overline{\mu}_J$ is the constant viscosity coefficient and λ is the ratio of relaxation to retardation times (Jeffrey fluid parameter). The velocity of blood can be obtained by solving Eq.(1) with the boundary conditions given as follows:

$$\frac{d\overline{u}}{d\overline{r}} \text{ is finite at } \overline{r}=0 \tag{2}$$

$$\overline{u}=\overline{u}_s \text{ at } \overline{r}=\overline{R}(\overline{z}), \tag{3}$$

where $\overline{R}(\overline{z})$ is the artery radius at the stenosed location given as (18)

$$\overline{R}(\overline{z})=\overline{R}_0-\frac{\overline{\delta}_h}{2}\left\{1+\cos\left(\frac{2\pi}{\overline{L}_0}\left(\overline{z}-\overline{d}-\frac{\overline{L}_0}{2}\right)\right)\right\}, \overline{d}\le\overline{z}\le\overline{L}_0+\overline{d}, \tag{4}$$

where $\overline{\delta}_h$, $\overline{d}$, and $\overline{L}_0$ are the stenosis height, stenosis location and solute length. Then, the momentum equation in this study is given by (5) and it is defined as follows:

$$\frac{d\overline{p}}{d\overline{z}}=-\frac{1}{\overline{r}}\frac{\partial}{\partial\overline{r}}(\overline{r}\overline{\tau}), \tag{5}$$

where $\overline{p}$ is the fluid pressure. The applied pressure gradient along the axial direction given by (5) is defined as follows:

$$\frac{d\overline{p}}{d\overline{z}}=-\overline{q}_0 p_s \tag{6}$$

where p_s refers to the non-dimensional steady state pressure gradient, while $\overline{q}_0$ corresponds to the negative pressure gradient within the normal artery region. The two-dimensional unsteady convective-diffusion equation is subsequently given by (17):

$$\frac{\partial\overline{C}}{\partial\overline{t}}+\overline{u}(\overline{r})\frac{\partial\overline{C}}{\partial\overline{z}^*}=\overline{D}_m\left(\overline{\nabla}^2+\frac{\partial^2}{\partial\overline{z}^{*2}}\right)\overline{C}, \tag{7}$$

where $\overline{C}$ represents the concentration of solute, $\overline{t}$ denotes the time, $\overline{D}_m$ is the molecular diffusion, $\overline{z}^*$ indicates the axial direction for solute concentration and

$$\overline{\nabla}^2=\frac{1}{\overline{r}}\frac{\partial}{\partial\overline{r}}\left(\overline{r}\frac{\partial}{\partial\overline{r}}\right). \tag{8}$$

Based on the Eq. (7), the initial boundary condition is respectively given by (17)

$$\overline{C}(\overline{r},\overline{z}^*,0)=\begin{cases}\overline{C}_o, \text{ if } |\overline{z}^*|\le\frac{\overline{z}_s}{2},\\ 0, \text{ if } |\overline{z}^*|>\frac{\overline{z}_s}{2},\end{cases} \tag{9}$$

with $\overline{C}_0$ representing the reference concentration and $\overline{z}_s$ denoting the solute length. The boundary condition of the Eq. (7) in the context of axial distribution is also given by (17)

$$\overline{C}(\overline{r},\infty,\overline{t})=0. \tag{10}$$

The symmetry boundary condition of the Eq. (7) at the center of the circular pipe center $\overline{r}=0$ is expressed as

$$\frac{\partial\overline{C}}{\partial\overline{r}}(0,\overline{z}^*,\overline{t})=0 \tag{11}$$

and the boundary condition of the Eq. (7) at the wall, $\overline{r}=\overline{R}(\overline{z})$ is given by

$$\frac{\partial\overline{C}}{\partial\overline{r}}(\overline{R}(\overline{z}),\overline{z}^*,\overline{t})=0. \tag{12}$$

Non-dimensional Variables

Take into account the following non-dimensional variables:

$$\tau=\frac{\overline{\tau}}{\overline{q}_0\overline{R}_0/2}, r=\frac{\overline{r}}{\overline{R}_0}, R(z)=\frac{\overline{R}(\overline{z})}{\overline{R}_0}, u=\frac{\overline{u}}{\overline{q}_0\overline{R}_0^2/4\overline{\mu}_J}, u_s=\frac{\overline{u}_s}{\overline{q}_0\overline{R}_0^2/4\overline{\mu}_J}, C=\frac{\overline{C}}{\overline{C}_0},$$
$$t=\frac{\overline{D}_m\overline{t}}{\overline{R}_0^2}, z^*=\frac{\overline{D}_m\overline{z}^*}{\overline{R}_0^2(\overline{q}_0\overline{R}_0^2/4\overline{\mu}_J)}, \delta_h=\frac{\overline{\delta}_h}{\overline{R}_0}, d=\frac{\overline{d}}{\overline{L}}, L_0=\frac{\overline{L}_0}{\overline{L}}, z=\frac{\overline{z}}{\overline{L}} \tag{13}$$

where τ, r, $R(z)$, u, u_s, C, t, z^*, Pe, δ_h, d, L_0 and z are the shear stress, artery radius, artery radius at the stenosed location, velocity, slip velocity, concentration of solute, time, axial distance for solute concentration, Peclet number, stenosis height, stenosis location, solute length and axial distance for blood flow in non-dimensional form.

Method of Solution

By using non-dimensional variables Eq.(13) in Eqs.(1)-(5), the equations become

$$\tau = -\frac{1}{2(1+\lambda)}\frac{du}{dr}, 0 \le r \le R(z), \tag{14}$$

$$\frac{du}{dr} \text{ is finite at } r = 0, \tag{15}$$

$$u = u_s \quad \text{at} \quad \bar{r} = \bar{R}(\bar{z}), \tag{16}$$

$$R(z) = 1 - \frac{\delta_h}{2}\left\{1 + \cos\left(\frac{2\pi}{L_0}\left(z - d - \frac{L_0}{2}\right)\right)\right\}, d \le z \le L_0 + d. \tag{17}$$

$$2P_s = -\tfrac{1}{r}\tfrac{\partial}{\partial r}(r\tau). \tag{18}$$

Substituting Eq. (13) into Eq. (7) yields

$$\frac{\partial C}{\partial t} + u(r)\frac{\partial C}{\partial z} = \left(l^2 + \frac{1}{(Pe)^2}\frac{\partial^2}{\partial z^2}\right)C \tag{19}$$

where

$$l^2 = \frac{1}{r}\frac{\partial}{\partial r}\left(r\frac{\partial}{\partial r}\right), \tag{20}$$

and P_e is given by (15) as follows:

$$Pe = \frac{\bar{q}_0 \bar{R}_0^3}{4\bar{\mu}_f \bar{D}_m}. \tag{21}$$

Solving Eq.(18) to obtain the shear stress τ, substituting into Eq.(14) and solving Eq.(14) using the boundary conditions in Eq.(15) and Eq.(16), the velocity of blood flow is obtained as

$$u(r) = Ps(1+\lambda)r^2 + u_s - Ps(1+\lambda)R^2(z). \tag{22}$$

The mean velocity of Jeffrey fluid in a stenosed artery is obtained as

$$u_m = u_s - \frac{1}{2}Ps(1+\lambda)R^2(z). \tag{23}$$

A new coordinate system (r, z_1, t) is introduced, with the new axial coordinate z_1 corresponding to the convection of solute across a plane moving with the mean velocity of the fluid, where the axis itself moves with the fluid's mean velocity

$$z_1 = z^* - u_m t. \tag{24}$$

Applying the approach from (17), the solution of Eq.(19) is expressed as a derivative series expansion as follows:

$$C(r, z_1, t) = C_m(z_1, t) + \sum_{i=1}^{\infty} f_i(r,t)\frac{\partial^i C_m(z_1,t)}{\partial z_1^i}, \tag{25}$$

where

$$C_m(z_1,t) = \frac{2}{R^2(z)}\int_0^{R(z)} C(r, z_1, t) r dr \tag{26}$$

denotes the mean solute concentration over the geometry's cross-sectional area.

Generalized Dispersion Model

The entire dispersion process can be described by the Generalized dispersion model (GDM). This is including the dispersion coefficient and how the dispersion process changes depending on time. By applying Eq.(26) and multiplying Eq.(19) by $2r$ before integrating with the respect to r, the Generalized Dispersion Model for $C_m(z_1,t)$ is expressed by

$$\frac{\partial C_m}{\partial t}(z_1,t) = \sum_{i=1}^{\infty} K_i(t)\frac{\partial^i C_m}{\partial z_1^i}(z_1,t), \tag{27}$$

where $K_i(t)$ denotes the transport coefficient specified by

$$K_i(t) = \frac{\partial_{i2}}{\partial t} + 2\frac{\partial f_i}{\partial r}(1,t) - 2\int_0^{R(z)} f_{i-1}(r,t)u(r)r\,dr, \quad i = 1,2,3,.. \tag{28}$$

with representing the longitudinal convection coefficient is $K_1(t)$ and the longitudinal diffusion coefficient is $K_2(t)$ represents the coefficient the effective axial diffusivity in the overall dispersion process for a simple diffusion scenario. For Newtonian fluids, the value of $K_3(t)$ is negligibly small, $K_3(t \to \infty) = -1/23040$ so the terms involving $K_3(t)$, $K_4(t)$, $K_5(t)$ and similar coefficients are disregarded. To evaluate $\frac{\partial C_m}{\partial t}$ and grouping the coefficient of $\frac{\partial^i C_m}{\partial z_1^i}$, $i = 1,2,3,...$ together to obtain, it yields

$$\begin{aligned}&\left[\frac{\partial f_1}{\partial t} - l^2 f_1 + u - u_m + K_1(t)\right]\frac{\partial C_m}{\partial t} + \\ &\left[\frac{\partial f_2}{\partial t} - l^2 f_2 + (u-u_m)f_1 + K_1(t)f_1 + K_2(t) - \frac{1}{Pe^2}\right]\frac{\partial^2 C_m}{\partial z_1^2} + \\ &\sum_{i=1}^{\infty}\left[\frac{\partial f_{i+2}}{\partial t} - l^2 f_{i+2} + (u-u_m)f_{i+2} - \frac{1}{Pe^2}f_i + \sum_{j=1}^{i+1} K_j(t) f_{i+2-j} + \right]\frac{\partial^{i+2} C_m}{\partial z_1^{i+2}} =\end{aligned} \tag{29}$$

By equating the coefficient of $\frac{\partial^i C_m}{\partial z_1^i}$ to zero for i=1,2,3 in Eq.(29), the following of infinite system of partial differential equation is given by

$$\frac{\partial f_1}{\partial t} - l^2 f_1 + u - u_m + K_1(t) = 0, \tag{30}$$

$$\frac{\partial f_2}{\partial t} - l^2 f_1 + \left[u - u_m + K_1(t)\right]f_1 + K_2(t) - \frac{1}{Pe^2} = 0, \tag{31}$$

and

$$\frac{\partial f_2}{\partial t} - l^2 f_{i+2} + \left[u - u_m + K_1(t)\right] f_{i+1} + \left(K_2(t) - \frac{1}{Pe^2}\right) f_i + \sum_{j=1}^{i+2} K_j(t) f_{i+2-j} = 0 \quad (32)$$

for $i = 1, 2, 3, \ldots$

From Eq.(25), $C(r,z_1,t)$ is expressed in term of $C_m(z_1,t)$,so $C_m(z_1,t)$ can be chosen to satisfy the initial boundary of $C(r,z_1,t)$ and it is implied that f_1 following the initial boundary conditions must be satisfied by

$$f_i(r,0) = 0, \quad (33)$$

$$\frac{\partial f_i}{\partial r}(0,t) = 1, \quad (34)$$

$$\frac{\partial f_i}{\partial r}(R(z),t) = 0, \quad (35)$$

respectively. Using Eq.(27), it yields

$$C_m(z_1,t) = C_m(z_1,t) + 2\sum_{i=2}^{\infty} f_i(r,t) r dr \frac{\partial C_m(z_1,t)}{\partial z_1^i}. \quad (36)$$

Comparing both sides in Eq.(36), it shows that the term of $\frac{\partial^i C_m}{\partial z_1^i}$ on the left hand side is zero and thus solvability condition is obtained as (18)

$$\int_0^{R(z)} f_i r dr = 0. \quad (37)$$

By performing the multiplication of Eq.(32) by r and integrating the resulting equation between zero and one with respect to r, and then applying Eq.(37), the longitudinal convection coefficient is obtained in the form of

$$K_1(t) = -2\int_0^{R(z)} (u - u_m) r dr = 0. \quad (38)$$

Following the procedure outlined in Eq.(31) and Eq.(32), the corresponding transport coefficients are defined as

$$K_2(t) = \frac{1}{Pe^2} - 2\int_0^{R(z)} f_1 u r dr \quad (39)$$

and

$$K_{i+2}(t) = -2\int_0^{R(z)} f_{i+1} u r dr, \ i = 1, 2, 3, \ldots. \quad (40)$$

Solution of Dispersion

The coefficient function, known as the dispersion function $f_i(r,t)$ is essential for quantifying the deviation of the local concentration $C(r,z_1,t)$ from the mean concentration $C_m(z_1,t)$. The solution of Eq.(30), which satisfies the boundary conditions from Eqs.(33)-(35), can be expressed into two parts (18) as shown in

$$f_1(r,t) = f_{1s}(r) + f_{1t}(r,t), \quad (41)$$

where $f_{1s}(r)$ represents the dispersion function in the steady state, and $f_{1t}(r,t)$ represents the dispersion function in the unsteady state, capturing the time-dependent nature of solute dispersion. Applying Eq.(38) and Eq.(41) in Eq.(30) yield

$$\frac{\partial f_{1s}}{\partial t} + \frac{\partial f_{1t}}{\partial t} - l^2(f_{1s} + f_{1t}) + (u - u_m) = 0. \quad (42)$$

After combining the $f_{1s}(r)$ and $f_{1t}(r,t)$ terms together and equating each to zero, the simplified differential equation for $f_{1s}(r)$ and $f_{1t}(r,t)$ are obtained. In the case of steady dispersion, the $\frac{\partial f_{1s}}{\partial t}$ term equal zero, resulting in the equations shown as

$$l^2 f_{1s} - (u - u_m) = 0 \quad (43)$$

and

$$\frac{\partial f_{1t}}{\partial t} = l^2 f_{1t}. \quad (44)$$

The initial condition of $f_{1t}(r,t)$ is given by

$$f_{1t}(r,0) = -f_{1s}(r) \quad (45)$$

and the boundary conditions of $f_{1s}(r)$ and $f_{1t}(r,t)$ are given by

$$\frac{df_{1s}}{dr}(0) = \frac{df_{1s}}{dr}(R(z)) = 0 \quad (46)$$

and

$$\frac{\partial f_{1t}}{\partial r}(0,t) = \frac{\partial f_{1t}}{\partial r}(R(z),t) = 0. \quad (47)$$

Equating the solvability of $f_{1s}(r)$ and $f_{1t}(r,t)$ and the following solvability conditions for $f_{1s}(r)$ and $f_{1t}(r,t)$ are as follow [(5) & (19)]

$$-\int_0^{R(z)} f_{1s} r dr = 0 \quad (48)$$

and

$$\int_0^{R(z)} f_{1t} r dr = -\int_0^{R(z)} f_{1s} r dr = 0. \quad (49)$$

By applying the boundary conditions in Eq.(46), the differential equation of dispersion function at the steady state in Eq.(43) becomes

$$f_{1s}(r) = \frac{P_z}{16}\left[r^4 + \lambda r^4 - (1+\lambda) 2 r^2 R^2(z)\right] + CI, \quad (50)$$

where

$$CI = \frac{P_z R^4(z)}{24}(1+\lambda) \quad (51)$$

Applying the method of variable separation and Bessel functions, the unsteady equation can be solved, yielding to the general solution, $f_{1t}(r,t)$ presented in

$$f_{1r}(r,t)=\sum_{m=1}^{\infty}A_m e^{-\lambda_m^2 t}J_0(\lambda_m r), \quad (52)$$

where λ_m's are the roots of the equation $J_1(\lambda_m) = 0$ where J_1 denotes the Bessel's functions of the first kind of order one and as defined as

$$A_m=-\frac{\int_0^{R(z)}J_0(\lambda_m r)f_{1z}(r)r\,dr}{\int_0^{R(z)}J_0^2(\lambda_m r)r\,dr}=-\frac{2}{J_0^2(\lambda_m)}\int_0^{R(z)}J_0(\lambda_m r)f_{1z}(r)r\,dr, \quad (53)$$

Since that the value of $K_3(t)$ for Newtonian fluid is extremely small $K_3(t\to\infty)$= - 1/23040 the terms $K_3(t)$, $K_4(t)$, $K_5(t)$ and similar ones are omitted by ignoring the coefficients involving them. Thus, Eq.(27) simplifies to

$$\frac{\partial C_m(z_1,t)}{\partial t}=K_2(t)\frac{\partial^2 C_m(z_1,t)}{\partial z_1^2}. \quad (54)$$

By using Inverse Fourier Transform (IFT), the solution of mean concentration of solute $C_m(z_1,t)$ in Eq.(54) is acquired as follows:

$$C_m(z_1,t)=\frac{1}{2}\left[erf\left(\frac{\frac{z_s}{2}-z_1}{2\sqrt{\xi}}\right)+erf\left(\frac{\frac{z_s}{2}+z_1}{2\sqrt{\xi}}\right)\right]. \quad (55)$$

RESULTS

The ratio of relaxation time, slip velocity and the relative height of stenosis on the blood velocity and unsteady dispersion function of solute through a stenosed artery are some of the characteristics who investigate in this study. The impacts of the relative height of stenosis and the ratio of relaxation time on the blood velocity and unsteady dispersion function of solute through a stenosed artery are indicates in Figures 2 - 7.

The parameter ranges outlined in this analysis are as follows: values of the radius of artery are $r = -1$ to 1, the slip velocity are u_s = 0. to 0.6, the time are t = 0 to 0.1, the relative height of stenosis are $\frac{\delta_s}{R_0}=0$ to 0.1 and the ratio of relaxation time are λ = 0 and 1.2. These results concentrated on the presence of Jeffrey fluid parameter within a stenosed artery.

Velocity of Blood Flow

The velocity of Jeffrey fluid with the effect of stenosis is illustrated in Figure 2 and the result has been validated with (18). Figures 3 and 4 shows the variation of velocity, u for different values of slip velocity, u_s in the blood flow through stenosed artery without and with the presence of the ratio of relaxation time, λ. In the presence of the ratio of relaxation time in Figure 4, it enhances the velocity of blood flow compared to the velocity in Figure 3.

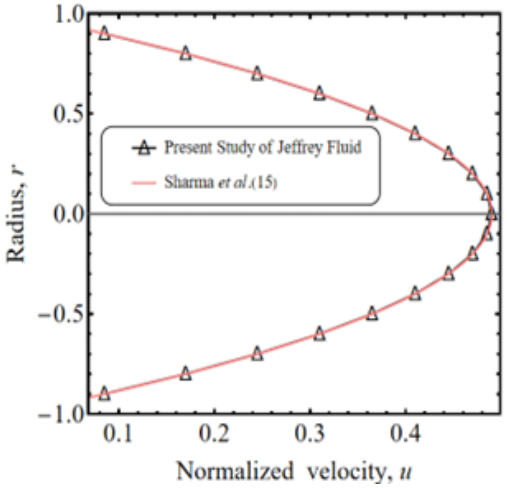

Fig 2: Validation of present velocity with Sharma et al. (15).

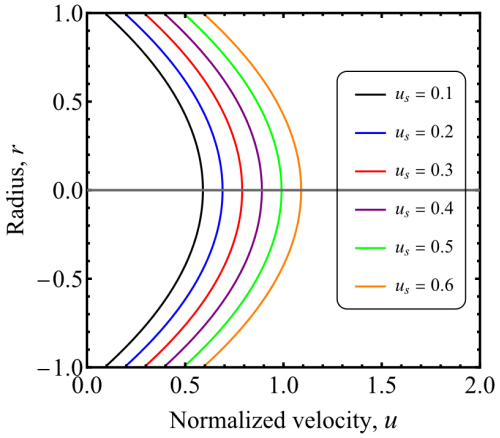

Fig 3: Variation of velocity, u for different values of slip velocity, u_s in the blood flow through a stenosed artery without the ratio of relaxation time, λ

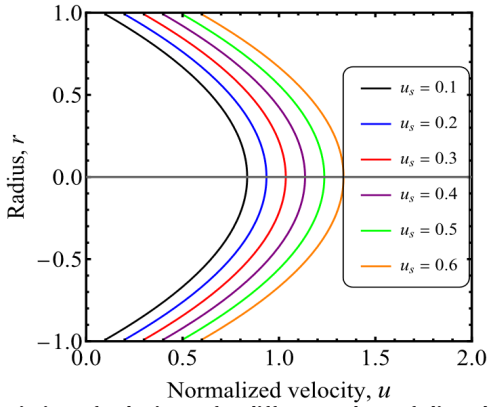

Fig 4: Variation of velocity, u for different values of slip velocity, u_s in the blood flow through a stenosed artery with the presence of the ratio of relaxation time, λ

A longer relaxation time means the blood resists deformation for longer period after shear stress applied, leading to a more uniform velocity (20). In high relaxation time, the shear strain remains significant and the blood

more elastically to maintain its deformation as the velocity gradient reduces (21). The relaxation behavior of viscoelastic fluid can be influenced by an increase in slip velocity. The relaxation time and slip velocity are combined to create a dynamic system, balancing elastic recoil with viscous dissipation. Higher relaxation time and enhanced slip velocity influence how blood cells carriers are transported and adhere to vessels walls. This can be leveraged in designing therapies for cancer or localized drug delivery.

Unsteady Solute Dispersion Function

Figure 5 shows the variation of unsteady dispersion function, f_{1t} for different values of time, t in the blood flow through stenosed artery without the presence of the ratio of relaxation time, λ . Based on the figure, the unsteady dispersion function, f_{1t} decreases at the center of artery and the dispersion are increases at the wall as the time are increases. It also shows that at time, t = 0 the unsteady dispersion function, f_{1t} exhibits the optimum outcome and when time, t increases until the value of t = 0.1, the unsteady dispersion function, f_{1t} decreases at the center. While at the wall of arteries, the unsteady dispersion function, increase as the time, increases.

Figure 6 shows the variation of unsteady dispersion function, f_{1t} for different values of time, t in the blood flow through stenosed artery with the presence of the ratio of relaxation time, λ Based on the figure, the unsteady dispersion function, f_{1t} significant decreases at the center of artery and the dispersion are increases at the wall as the time are increases. It also shows that at time $t = 0$, the unsteady dispersion function, f_{1t} exhibits the optimum outcome and when time, t increases until the value of t = 0.1 , the unsteady dispersion function, decreases at the center. While at the wall of arteries, the unsteady dispersion function, f_{1t} increase as the time, t increases. The presence of the ratio of relaxation time, λ affects the dispersion function significantly. While, in the presence of the ratio of relaxation time in Figure 6, it enhances the unsteady dispersion function compared to the unsteady dispersion function in Figure 5. The presence of the ratio of relaxation time affects the unsteady dispersion function especially at the center and at the wall of the artery. The presence of the ratio of relaxation time enhanced time-dependent effects, delaying or oscillating particle to spread in the artery. Copley et al. (22) noted that blood with a longer relaxation period tends to flow more uniformly in steady flow, resulting in fewer velocity gradients. This behavior may have consequences for solute dispersion in arterial systems (5). Longer relaxation times delay the drug's uniform distribution, requiring tailored delivery methods to ensure effective dispersion.

Figure 7 illustrates the unsteady dispersion function, f_{1t} varies with different relative heights of stenosis profile, $\frac{\delta_h}{R_0} = 0$ in the blood flow through a stenosed artery, considering presence of the ratio of relaxation time, λ. According to the figure, as the relative height of the stenosis profile increases, the unsteady dispersion function, f_{1t} significantly decreases at the center of the artery and increases at the wall. The inclusion of the relaxation time ratio, λ greatly influences the dispersion

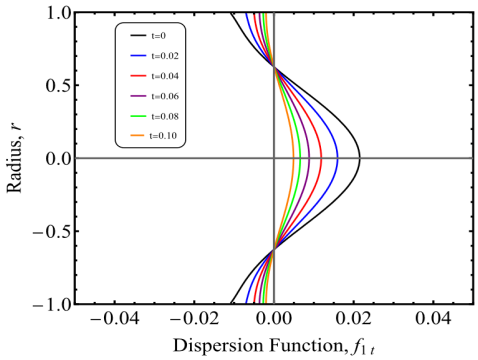

Fig 5: Variation of unsteady dispersion function, f_{1t} for different value of time, t in the blood flow through stenosed artery without the ratio of relaxation time, λ

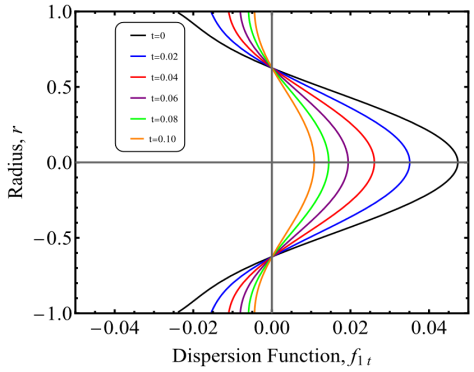

Fig 6: Variation of unsteady dispersion function, f_{1t} for different value of time, t in the blood flow through stenosed artery with the ratio of relaxation time, λ

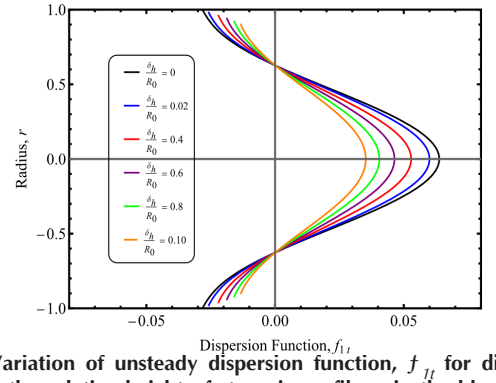

Fig 7: Variation of unsteady dispersion function, f_{1t} for different value of the relative height of stenosis profile, t in the blood flow through stenosed artery with the ratio of relaxation time, λ .

function by causing a substantial rise in the unsteady dispersion function.

DISCUSSION

The goal of this study is to explore the impacts of various parameters, such as the relative height of stenosis profile, slip velocity and the ratio of relaxation time on the velocity of blood flow and the unsteady dispersion function within a stenosed artery. This study intends to investigate the impact of various factors on blood flow behavior via simulations and to contrast the results with the findings of current research. The focus of the discussion is on the variations in velocity and the unsteady dispersion function across various conditions, highlighting the significant role of the relaxation time ratio in determining blood flow velocity and its notable effect on the dispersion function. The findings observed that factors such as ratio of relaxation time, slip velocity and the relative height of stenosis play crucial roles in shaping the flow characteristics within the artery, with implications for understanding blood flow dynamics in stenosed arteries.

Velocity of Blood Flow

This section examines the way of velocity changes in response to variation in relaxation time ratio and the relative height of stenosis within stenosed artery. Figure 2 shows a good agreement with (18). The results obtained are consistent with those in references (18) when the radius of the artery in the stenosed core region is set to zero. In (18), the study discussed about two-layered Jeffrey-fluid model with mild stenosis in narrow tubes while the present study examines about single-layered Jeffrey-fluid by evaluate the consequences of the ratio of relaxation time, slip velocity and the relative height of stenosis within a stenosed artery towards the blood velocity and solute dispersion. Depending on the study's focus, both the two-layer and single Jeffrey fluid models have special advantages and are appropriate for various applications.

The single Jeffrey fluid model is effective for investigating small-scale flows, micro vessels, or low-hematocrit situations because it captures the viscoelastic characteristic of blood and produces smooth velocity profiles. It focuses on simpler velocity changes and is computationally simpler.

The variation in velocity, u for different slip velocities, u_s in blood flow through a stenosed artery as depicted in Figures 3 and 4, showing scenarios with and without the relaxation time ratio, λ. The existence of the relaxation time ratio, λ when λ =1.2 rise the velocity of blood flow in Figure 4 compared to Figure 3 when λ =0. Furthermore, an increase in slip velocity, increase the velocity. Thus, when blood has a higher relaxation time, it implies a slower relaxation response to changes in velocity gradients. This slower relaxation response may lead to enhanced slip at the wall and resulting in a larger slip velocity.

Unsteady Solute Dispersion Function

This section examines the way unsteady dispersion changes in response to variation in relaxation time ratio and the relative height of stenosis within stenosed artery. In present study, the study examined the process of the drug are dispersed in Jeffrey blood flow within time-dependent compared to (18) which did not address the dispersion of solutes within the flow. The study of unsteady solute dispersion is conducted to understand and analyze the drug molecules, disperse in blood flow under time dependent. The variation of unsteady dispersion function, f_{1t} for different values of time, t in the blood flow through a stenosed artery is depicted in Figures 5 and 6, highlighting conditions both with and without the relaxation time ratio, λ. According to the figure, the unsteady dispersion function, f_{1t} reduces at the artery's center and grows at the wall with increasing time. In the presence of the ratio of relaxation time, λ presence when $\lambda = 1.2$ the unsteady dispersion function, f_{1t} shown in Figure 6 is much larger compared to that in Figure 5 when $\lambda = 0$. It also indicates that at time, $t = 0$ the unsteady dispersion function, achieve its optimal result, and as time, t increases until the value of $t = 0$, the value unsteady dispersion function, f_{1t} decreases at the center. Meanwhile, at the arterial wall, the unsteady dispersion function, f_{1t} rise as time progresses. This study of unsteady dispersion can be applied to evaluate the effectiveness of drug delivery in blood flow. When the drug (medicine) is injected into blood vessels, the particles of drug are dispersed in the artery within time dependent. In the present of the ratio of relaxation time, the drug (medicine) takes time to disperse in the artery and balance between elastic and viscous behaviors (5). According to Figure 7, as the relative height of the stenosis profile increases, the unsteady dispersion of the drug (medicine) in the blood flow significantly decreases at the center because of the blood vessels lumen become narrow due to stenosis. The drug (medicine) dispersed slowly to pass through a blood vessel with the stenosis at the center and the time taken becomes longer because

of the ratio of relaxation time and creates a higher concentration upstream of the stenosis (23).

Additionally, there are also real-world practical applications for the findings. For instance, optimizing medication delivery systems for targeted treatments, like stent-based drug release, can be improved by the understanding of solute dispersion in stenosed arteries. Moreover, the findings could impact the development of diagnostic techniques like contrast substance dispersion imaging that depend on solute transport data.

This study could be further upon in the future by examining deeper and relevant cases. For example, a deeper understanding of solute transport in curved or branching arteries could potentially be possible by extending the model to three-dimensional (3D) geometries. Analysis of artery wall resistance and its impact on solute dispersion would be possible with the inclusion of fluid-structure interaction (FSI). The applications of fluid-structure interaction (FSI) in mechanical and biological engineering have drawn a lot of interest from scientists and researchers (24). Additionally, simulating the accumulation and development of low-density lipoprotein (LDL) in stenosed areas may provide important information about the atherosclerosis development.

CONCLUSION

A mathematical model has been created and employed to investigate the concept of dispersion solute, focusing on unsteady solute dispersion in Jeffrey fluid. In this study, the influence of both the relaxation time ratio and the relative height of the stenosis profile on solute dispersion in a stenosed artery's blood flow is analyzed by using the Jeffrey fluid model.

According to the results, increasing the ratio of relaxation time leads to higher flow velocity. Regarding the unsteady dispersion function, it decrease at the center of the artery while increasing at the wall as time goes on. The presence of the relaxation time ratio causes a significant rise in unsteady dispersion at the artery's center and a marked decrease at the wall. An increase in the relative height of the stenosis profile leads to a decrease in the unsteady dispersion function With the inclusion of the relaxation time ratio, the unsteady dispersion function significantly rises at the artery's center and decreases markedly at the wall, as the relative height of the stenosis profile is adjusted.

The findings of this study are advantageous for researchers seeking a deeper understanding of how the ratio of relaxation time and the relative height of stenosis influence blood flow and solute dispersion. Hence, the present findings in this study provide a clear understanding into the issues of arteries and drug dispersion with stenosis and improve the treatment of CVD. The insights gained from the study of Jeffrey fluid, in relation to the ratio of relaxation time and the relative height of stenosis, are advantageous for predicting drug delivery to particular stenosed regions affected by abnormal plaque, enabling more precise and targeted therapeutic approaches. By determining the dispersion function, healthcare professionals can tailor treatment strategies to the unique characteristics of each stenosed area. This optimization leads to more effective and efficient treatment outcomes.

To advance practical understanding, future investigations should explore solute dispersion in arterial blood flow. Additionally, it is advisable for future research on Jeffrey fluid to examine how different viscosities affect the ratio of retardation time.

ACKNOWLEDGEMENT

This research was supported by Ministry of Education (MOE) Malaysia through Fundamental Research Grant Scheme (FRGS) (FRGS/1/2020/STG06/UTM/02/15) and Universiti Teknologi Malaysia, UTMFR, PY/2024/01517/Q.J130000.3854.23H98.

REFERENCES

1. Ellahi, R., Rahman, S. U., & Nadeem, S. (2014). Blood flow of Jeffrey fluid in a catherized tapered artery with the suspension of nanoparticles. Physics Letters, Section A: General, Atomic and Solid State Physics, 378(40), 2973–2980. https://doi.org/10.1016/j.physleta.2014.08.002
2. Kahshan, M., Lu, D., & Siddiqui, A. M. (2019). A Jeffrey Fluid Model for a Porous-walled Channel: Application to Flat Plate Dialyzer. Scientific Reports, 9(1). https://doi.org/10.1038/s41598-019-52346-8
3. Afsar Khan, A., Ellahi, R., & Vafai, K. (2012). Peristaltic transport of a Jeffrey fluid with variable viscosity through a porous medium in an asymmetric channel. Advances in Mathematical Physics. https://doi.org/10.1155/2012/169642
4. Priyadharshini, S., & Ponalagusamy, R. (2017).

Computational model on pulsatile flow of blood through a tapered arterial stenosis with radially variable viscosity and magnetic field. Sadhana Academy Proceedings in Engineering Sciences, 42(11), 1901–1913. https://doi.org/10.1007/s12046-017-0734-5

5. Chauhan, S. S., & Tiwari, A. (2022). Solute dispersion in non-Newtonian fluids flow through small blood vessels: A varying viscosity approach. European Journal of Mechanics, B/Fluids, 94, 200–211. https://doi.org/10.1016/j.euromechflu.2022.02.009
6. Akbar, N. S., & Nadeem, S. (2014). Carreau fluid model for blood flow through a tapered artery with a stenosis. Ain Shams Engineering Journal, 5(4), 1307–1316. https://doi.org/10.1016/j.asej.2014.05.010
7. Yan, S. R., Zarringhalam, M., Toghraie, D., Foong, L. K., & Talebizadehsardari, P. (2020). Numerical investigation of non-Newtonian blood flow within an artery with cone shape of stenosis in various stenosis angles. Computer Methods and Programs in Biomedicine, 192. https://doi.org/10.1016/j.cmpb.2020.105434
8. Dhange, M., Sankad, G., Safdar, R., Jamshed, W., Eid, M. R., Bhujakkanavar, U., Gouadria, S. & Chouikh, R. (2022). A mathematical model of blood flow in a stenosed artery with post-stenotic dilatation and a forced field. Plos one, 17(7), e0266727.
9. Munir, I. D., Jaafar, N. A., & Shafie, S. (2024). Solute dispersion in hemodynamic within a stenotic artery experiencing arterial inclination and body acceleration. In AIP Conference Proceedings (Vol. 3189, No. 1). AIP Publishing.
10. Dhange, M., Sankad, G., Bhujakkanavar, U., Das, K. K., & Misra, J. C. (2024). Hemodynamic characteristics of blood flow in an inclined overlapped stenosed arterial section. Partial Differential Equations in Applied Mathematics, 11, 100829.
11. Shukla, J. B., Parihar, R. S., & Rao, B. R. P. (1980). Effects of stenosis on non-Newtonian flow of the blood in an artery. Bulletin of mathematical biology, 42, 283-294.
12. Hussain, A., Sarwar, L., Akbar, S., & Malik, M. Y. (2022). Mathematical analysis of mass and heat transfer through arterial stenosis. Journal of Power Technologies, 102(3), 88-95.
13. Owasit, P., & Sriyab, S. (2021). Mathematical modeling of non-Newtonian fluid in arterial blood flow through various stenoses. Advances in Difference Equations, 2021(1). https://doi.org/10.1186/s13662-021-03492-9
14. Ratchagar, N. P., & Vijayakumar, R. (2020). Dispersion of a solute in a couple stress fluid with chemical reaction using generalized dispersion model. Advances in Mathematics: Scientific Journal, 9(4), 2233–2247. https://doi.org/10.37418/amsj.9.4.85
15. Singh, S., & Murthy, P. V. S. N. (2022). Unsteady solute dispersion in pulsatile Luo and Kuang blood flow (K - L Model) in a tube with wall absorption. Journal of Non-Newtonian Fluid Mechanics, 104928. https://doi.org/10.1016/j.jnnfm.2022.104928
16. Das, P., Sarifuddin, Rana, J., & Kumar Mandal, P. (2022). Unsteady solute dispersion in the presence of reversible and irreversible reactions. Proceedings of the Royal Society A: Mathematical, Physical and Engineering Sciences, 478(2264). https://doi.org/10.1098/rspa.2022.0127
17. Gill, W. N., & Sankarasubramanian, R. (1970). Exact analysis of unsteady convective diffusion. Proceedings of the Royal Society of London. A. Mathematical and Physical Sciences, 316(1526), 341-350.
18. Sharma, B. D., Yadav, P. K., & Filippov, A. (2017). A Jeffrey-fluid model of blood flow in tubes with stenosis. Colloid Journal, 79(6), 849–856. https://doi.org/10.1134/S1061933X1706014X
19. Jaafar, N. A., ZainulAbidin, S. N. A. M., Ismail, Z., & Mohamad, A. Q. (2021). Mathematical Analysis of Unsteady Solute Dispersion with Chemical Reaction Through a Stenosed Artery. Journal of Advanced Research in Fluid Mechanics and Thermal Sciences, 86(2), 56–73. https://doi.org/10.37934/arfmts.86.2.5673
20. Thurston, G. B. (1972). Viscoelasticity of human blood. Biophysical journal, 12(9), 1205-1217.
21. Bird, R.B., Armstrong, R.C., & Hassager, O. (1987). Dynamics of Polymeric Liquids, Vol. 1: Fluid Mechanics. 2nd ed. Wiley-Interscience.
22. Copley, A. L., King, R.G., Chien, S. , Usami, S., Skalak R. & Huang, C.R. (1975). Microscopic observations of viscoelasticity of human blood in steady and oscillatory flow, Biorheology 12, 257–263.
23. Mazumdar, J. (1999). An introduction to mathematical physiology and biology. Cambridge University Press, Pp13-18.
24. Shahzad, H., Wang, X., Ghaffari, A., Iqbal, K., Hafeez, M. B., Krawczuk, M., & Wojnicz, W. (2022). Fluid structure interaction study of non-Newtonian Casson fluid in a bifurcated channel having stenosis with elastic walls. Scientific Reports, 12(1), 12219.